PRESSURE EFFECT ON LUMINESCENCE OF INSULATING CRYSTALS DOPED WITH RARE EARTH IONS. EVIDENCE FOR TRAPPED EXCITON IN Pr^{3+} DOPED $LiNbO_3$ AND $LiTaO_3$

M. Grinberg and W. Gryk

Institute of Experimental Physics, University of Gdañsk, Wita Stwosza 57, 80-952 Gdañsk, Poland

Abstract. High pressure photoluminescence of $LiNbO_3$ and $LiTaO_3$ doped with Pr^{3+} is presented. Analysis of the emission at various pressures and temperatures allowed predicting existence of the Pr^{3+} trapped exciton consisted with ionized praseodymium Pr^{4+} and electron bound to the Coulomb potential of trapped hole. We have developed the exciton model and discussed configurational coordinate diagram of the system that explained pressure dependence of the energy of trapped exciton.

1. INTRODUCTION

Luminescent solid state insulating materials (normally oxides, chlorides, and fluorides) activated by rare earth ions are still the interesting objects of the research. The inorganic materials are desirable for practical applications for several reasons including mechanical strength, durability, chemical inertness, portability, easy chemical synthesis, and diversity of properties. The materials under consideration have potential application as solid state lasers, optical communications, scintillation, medical procedures, imaging, displays, flow cytometry, holography, and remote sensing, [1]. Specifically, the interest in crystals $LiXO_3$(X=Nb, Ta) results from their electrooptics and nonlinear properties [2,3]. Interest in doping with Pr^{3+} results from the broad spectral range of Pr^{3+} emission [3].

Rare earth dopand ions contribute to the energetic structure of the system by localized states (more than one) with energies above the valence band and below the conduction band of the host. It is a common practice to describe these states as belonging to $4f^n$ and $4f^{n-1}5d^1$($1 \le n \le 14$) electronic configurations of rare earth ion. Especially interesting are materials doped with Ce^{3+}, Pr^{3+}, and Eu^{2+} which have found application as scintillators, [4-6], and lasers, [7]. In these ions effective and useful luminescence results usually from the spin and parity allowed $4f^{n-1}5d^1 \rightarrow 4f^n$ transitions.

The emission wavelength depends on the energy of the lowest state of the $4f^{n-1}5d^1$ electronic configuration and extends from the yellow to UV region, [8-10]. In the commonly used approach this energy is related to the splitting of the of the 5d level; in the crystal field produced by the host near neighbor ions. In the case of Pr^{3+} and Eu^{2+} the $4f^{n-1}5d^1 \rightarrow 4f^n$ can be quenched by relaxation of the excitation to the excited states of the $4f^n$ electronic

Corresponding author: M. Grinberg, e-mail: fizmgr@univ.gda.pl

configuration and than the parity forbidden transitions inside the $4f^n$ shell.

For the some fluorite hosts MF_2 (M=Ca, Sr and Ba) the divalent rare earth ions doped into the lattice emit the broad band luminescence related to the impurity trapped exciton. This emission completes with normal $4f^{n-1}5d^1 \rightarrow 4f^n$ emission. Such anomalous excitonic luminescence has been observed in SrF_2:Yb^{2+}, [11,12], and BaF_2:Eu^{2+} [13], whereas normal $4f^6 5d^1 \rightarrow 4f^7$ emission has been observed in Eu^{2+} in SrF_2 [13] and CaF_2, [14].

As it has been mentioned, the energies of the states from the excited electronic configuration $4f^{n-1}5d^1$ are strongly dependent on the crystal field, whereas the states belonging to the $4f^n$ electronic configuration do not. Energies of localized levels of impurity trapped exciton are postulated to be related to the lattice properties (energy of the conduction band), [13,14].

The sensitivity of energy of d electrons on crystal field has caused the increasing of interests in application of high hydrostatic pressure to modify the energetic structure of rare earths doped crystals. The standard equipment is the optical high pressure cell with diamond (DAC) or sapphire anvils (SAC). High pressure spectroscopy has been extensively applied for the investigation of 3d-3d optical transitions in transition metal ions in solids (for review see [15] and [16]). The d-f transitions under pressure have been investigated by Tyner and Drickamer, [17] in Eu^{2+} doped $CaAl_2O_4$, $SrAl_2O_4$, $CaBPO_5$, $SrBPO_5$, $Ca_2P_2O_7$ and Ba_2SiO_4. They have observed the red shifts of the luminescence bands related to d-f emission in the range of 7-37 cm^{-1}/kbar. Paper [15] has reported pressure changes in luminescence lineshape and wavelength of $SrFCl$: Sm^{2+} system, caused by pressure induced decrease of the energy of $4f^5 5d^1$ electronic configuration. In the last years, high pressure has been used for investigation of the emission related to the $4f^{n-1}5d^1 \rightarrow 4f^n$ transitions, in the Ce^{3+} and Pr^{3+} ions in several materials, see [18-21] and [22-24], respectively. Yoo *et al.* [25] have investigated emission of Sm^{2+} in SrF_2 and have found the red shift of the $4f^5 5d^1 \rightarrow 4f^6$ emission band equal to -10 cm^{-1}/kbar. Summary of the available data is presented in [16]. As it has been discussed in paper [16] the energy of the lowest state of excited electronic configuration $4f^{n-1}5d^1$ decreases when pressure increases. There are almost no papers on investigation of anomalous, trapped exciton emission under high hydrostatic pressure. The only results obtained for BaF_2:Eu^{2+} and $Ba_{0.3}Sr_{0.7}F_2$:Eu^{2+}, [26],

show the red shift of anomalous emission by the order of -17 cm^{-1}/kbar and structural transition that transforms the emission lineshape from anomalous to normal $4f^5 5d^1 \rightarrow 4f^6$ luminescence at pressure 30 and 40 kbar for BaF_2:Eu^{2+} and $Ba_{0.3}Sr_{0.7}F_2$:Eu^2, respectively.

In this paper we present the high pressure spectroscopy results that evidence the existence of the Pr^{3+} trapped excitonic states in $LiNbO_3$ and $LiTaO_3$ crystals. We also present the theoretical model that allows predicting pressure induced shift of the excitonic emission spectrum.

2. EXPERIMENTAL METHOD AND RESULTS

Details of $LiTaO_3$:Pr^{3+} and $LiNbO_3$:Pr^{3+} crystals growing are described in our previous papers [27,28]. High pressure photoluminescence spectra have been measured at pressure from ambient to 232 kbar at 20K and room temperature. For high pressure application we have used the Merrill – Bassett, [29], diamond anvil cell (DAC). The poly (dimethylsiloxane) oil was used as pressure transmitting medium, and the small piece of ruby crystal has been used as pressure detector. Photoluminescence have been excited with the He-Cd laser (325 nm, 5 mW). Photoluminescence signal has been detected using PGS2 (Carl Zeiss Jena) spectrometer working as a monochromator and detected by the photomultiplier (Hamamatsu, R943-02) working in photon counting regime. The DAC has been cooled using the closed cycle helium cryostat (Cryogenics Inc, DE-202).

Typical emission spectra of the $LiNbO_3$:Pr^{3+} for selected pressures, obtained at room temperature are presented in Fig. 1. For pressure below 78 kbar, for all considered temperatures, we have only the sharp lines emission related to the $^1D_2 \rightarrow {}^3H_4$ and $^1D_2 \rightarrow {}^3H_5$ transitions, labeled in Fig. 1 by arrow 1 and 2, respectively. In our previous paper, [27] we have estimated the pressure shift of the $^1D_2 \rightarrow {}^3H_4$ emission to -2.35 cm^{-1}/kbar. Pressure shift of the $^1D_2 \rightarrow {}^3H_5$ transition has been found to be equal to -1.52 cm^{-1}/kbar. No emission from the higher excited state the $^3P_0$ is observed under 325nm excitation. When pressure increases above 78 kbar, apart of the sharp lines the broad band emission appears. We have measure the emission spectra for pressures 81, 92, 107, and 124 kbar at different temperatures. The spectra obtained at 81 kbar and 124 kbar are presented in Figs. 2a and 2b, respectively. Intensity of the broad band emission increases when temperature increases.
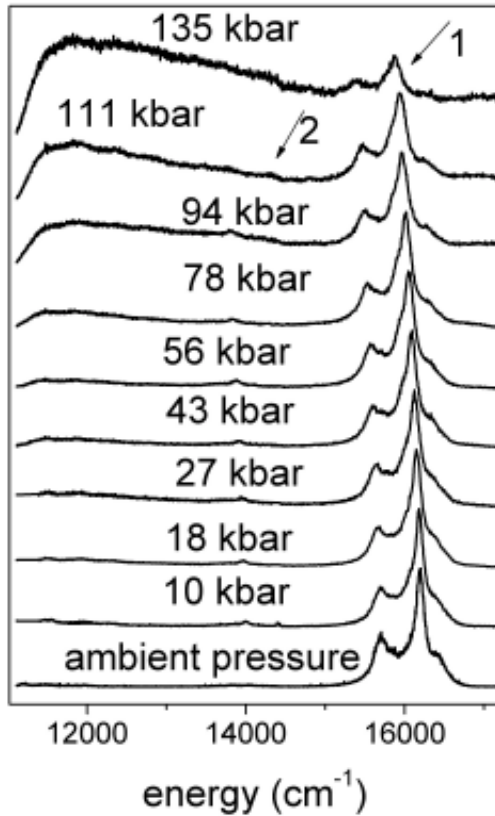
Fig. 1. $LiNbO_3$:Pr^{3+} emission spectra obtained for selected pressures at room temperature.

Fig. 2. $LiNbO_3$:Pr^{3+} emission spectra obtained at 81 kbar (a) and 124 kbar (b).

The relation between the broad band and sharp line luminescence can be understood in the meaning of the configurational coordinate diagram presented in Fig. 3. In the diagram the electronic manifolds related to Pr^{3+} states are labeled by $^3P_0$, $^1D_2$ and $^3H_4$. The solid curves labeled by $f^2+e^-+h^+$ represent the free electron and hole (bold) and free exciton (thin) system. The solid curves labeled by f^1+e^- represent ionized praseodymium ion and free electron and (bold) and impurity trapped exciton system (thin). The spectral lineshape at low temperature depends on that which state has lower energy; the trapped exciton (labeled $-E_{ex}$) or the $^1D_2$ state (labeled E_1). For $E_{ex} > E_1$ and $E_1 > E_{ex}$ we have the sharp lines related to $^1D_2 \rightarrow {}^3H_4$ transition and the broad band related to the trapped exciton recombination, respectively.

We have calculated the relative contributions of the broad band emission to the spectrum. The results obtained for different pressures are presented in Figs. 4a-4d. One should notice that for
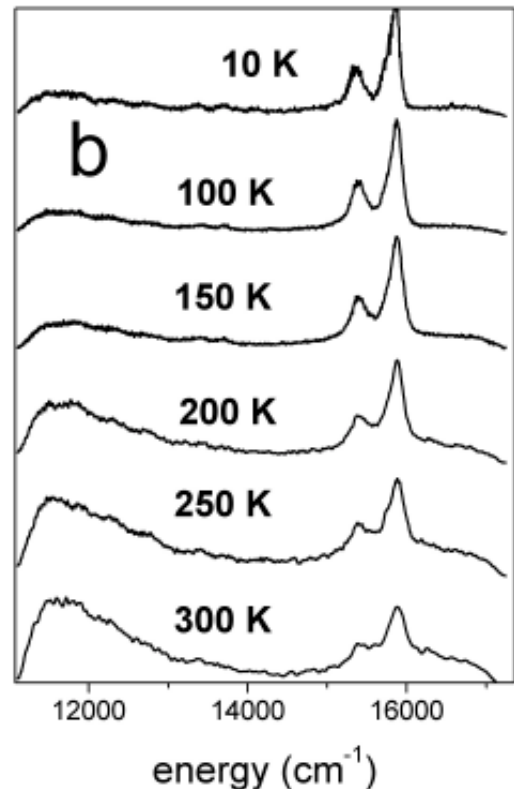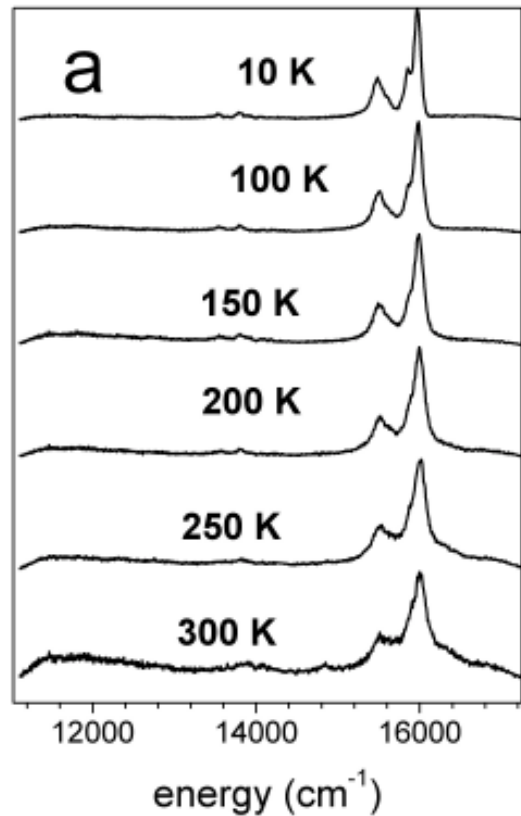
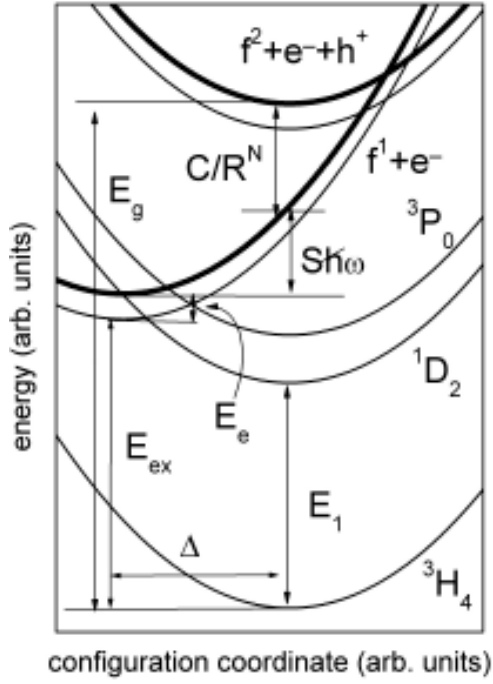**Fig. 3.** Configurational coordinate diagram describing trapped exciton in the $LiNbO_3{:}Pr^{3+}$, $LiTaO_3{:}Pr^{3+}$ systems.

considered pressures even for low temperature we have already both; the broad band and sharp lines luminescence. This effect is related to the inhomogeneous broadening of the trapped exciton system which results because in some sites $E_{ex} > E_1$ and in others $E_1 > E_{ex}$. This is a reason why we fitted our data to the following formula:

$$\frac{I_b(p,T)}{I_{tot}(p,T)} = \frac{I_b^0(p) + P_b^{eff} e^{\frac{-\Delta E_{eff}(p)}{kT}}}{I_s(p) + I_b^0(p) + P_b^{eff} e^{\frac{-\Delta E_{eff}(p)}{kT}}} \qquad (1)$$

and

$$\frac{I_s(p,T)}{I_{tot}(p,T)} = 1 - \frac{I_b(p,T)}{I_{tot}(p,T)}, \qquad (2)$$

where $I_b^0(p)$ and $I_s^0(p)$ is the intensity of emission from the sites where trapped exciton energy is lower than energy of the $^1D_2$ state and emission intensity form the sites with energy of trapped exciton grater than energy of the $^1D_2$ state, respectively. $P_b^{eff} e^{-\frac{\Delta E_{eff}(p)}{kT}}$ is additional broad band emission intensity from sites with thermally excited exciton
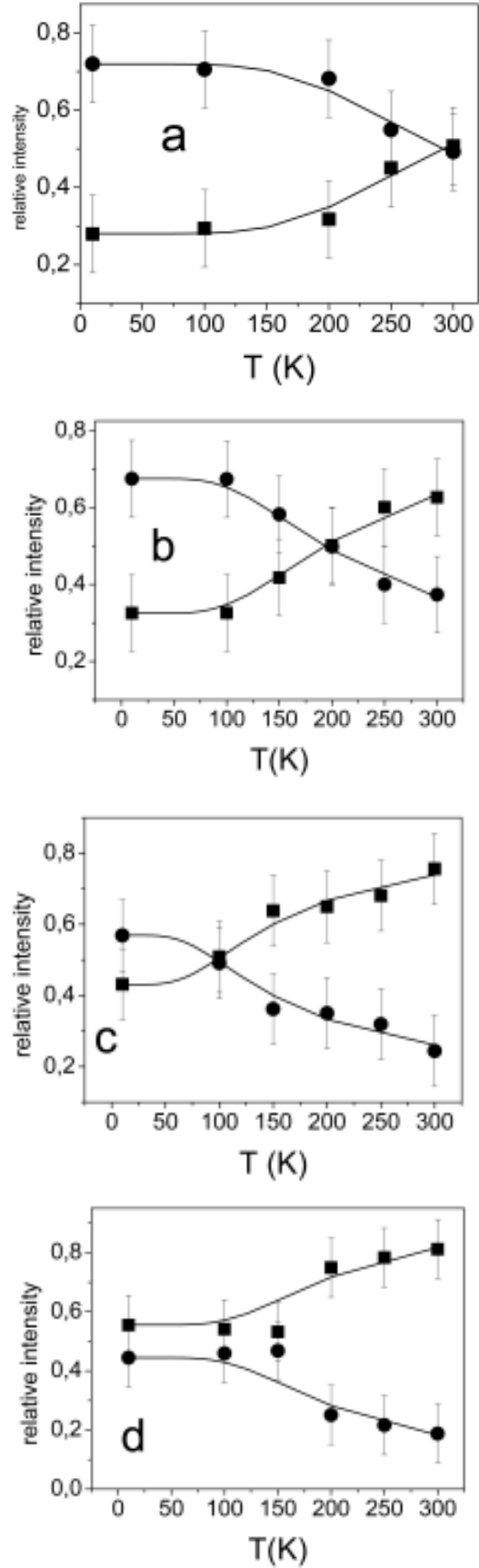
Fig. 4. The relative intensity of the broad band (rectangles) and sharp line (circles) versus temperature for pressure 81 kbar(a), 92 kbar (b), 107 kbar (c), and 124 kbar (d).

states. P_b^{eff} is the relative probability of exciton recombination. ΔE_{eff} is the effective energy of trapped exciton representing the sites which energy is greater than energy of the $^1D_2$ state, at given pressure. $I_b(p,T)$, $I_s(p,T)$ and $I_{tot}(p,T)$ are temperature dependent broad band exciton emission, sharp line $^1D_2 \rightarrow {}^3H_4$ emission and total emission intensity, respectively. Quantity $I_b^0(p)/I_s^0(p)$ can be directly estimated from the low temperature spectra as the intensity ratio of the sharp line to the broad band emission.

At pressure 81 kbar the intensity of the broad band becomes equal to the intensity of the sharp lines at temperature 300K. The temperature of crossover decreases when pressure increases, and at 124 kbar the broad band luminescence already dominates at 20K (see Figs. 4a-4d). One notices that crossover temperature decreases almost linearly with increasing pressure (with the rate $dT_{cross}/dp = -8K/kbar$). Relation (1) yields:

$$\frac{dT_{cross}}{dp} =$$

$$\frac{1}{k} \frac{d\Delta E_{eff} \left[\ln(P_b^{eff}) - \ln(I_s^0) - I_p^0(p) \right]}{dp}. \quad (3)$$

It is difficult to estimate P_b^{eff} and $\Delta_{eff}(p)$ independently. However one can consider that broad band emission is related to transitions from thermally occupied higher excited state related to Pr^{3+} trapped exciton which energy diminishes linearly with increasing pressure. Energy of the trapped exciton state in $LiNbO_3$:Pr^{3+} at ambient pressure is somewhere below energy of the $^3P_0$ state and above energy of the $^1D_2$ state of the Pr^{3+}. With increasing pressure this energy diminishes and at pressure above 130 kbar is smaller than energy of the $^1D_2$ state.

Quite similar effect has been observed in the case of $LiTaO_3$ doped with Pr^{3+}. In Fig. 5 low temperature emission spectra of the $LiTaO_3$:Pr^{3+} system at different pressures are presented. The luminescence consists of the sharp lines related to the $^1D_2 \rightarrow {}^3H_4$ transition (labeled by arrow 1) and to the $^3P_0 \rightarrow {}^3H_4$ transition (labeled by arrow 2). One observes pressure induced red shifts of these lines equal to -2.2 cm^{-1}/kabar and -2.5 cm^{-1}/kbar, respectively, [28]. The intensity of the $^3P_0 \rightarrow {}^3H_4$ transition quenches when pressure increases above 100 kbar. This effect is related to the nonradiative energy transfer from the $^3P_0$ state to the trapped exciton level and than to the $^1D_2$ state from which fi-
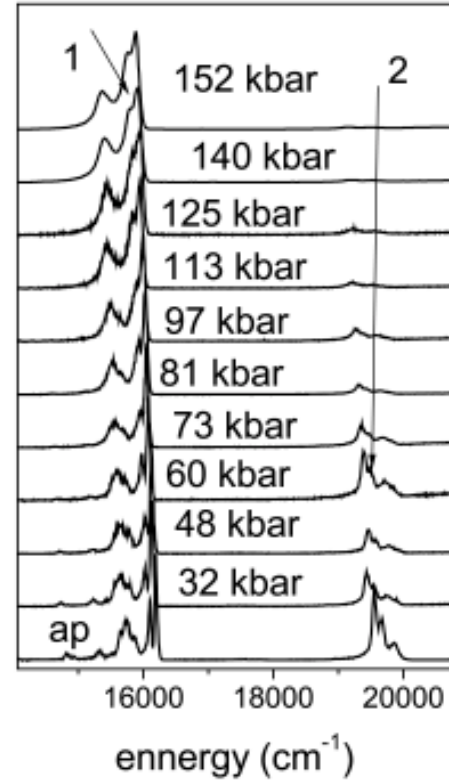

Fig. 5. $LiNbO_3$:Pr^{3+} emission spectra obtained for selected pressures at 20K.

nally emission occurs. The energy of the trapped exciton state in $LiTaO_3$:Pr^{3+} at ambient pressure is above the energy of the $^3P_0$ state. With increasing pressure this energy diminishes and at pressure above 100kbar is smaller than energy of the $^3P_0$, but still is much greater than energy of the $^1D_2$ state.

3. MODEL OF IMPURITY TRAPPED EXCITON

The configurational coordinate diagram representing the $LiTaO_3$:Pr^{3+} and $LiNbO_3$:Pr^{3+} system is presented in Fig. 3. To consider the energy of the $4f^2$ electronic manifold of the Pr^{3+} ion and the trapped exciton manifold, the following Hamiltonian has been proposed [28]

$$H = \frac{-\hbar^2 \nabla^2}{2m} + U_{loc}(\mathbf{r})|_{r<R} + V_{cr}(\mathbf{r}) - \frac{e^2}{\varepsilon \cdot r} + V_{latt}(\Delta), \quad (4)$$

where

$$U_{loc}(\mathbf{r})|_{r<R} = V_{RE}(\mathbf{r})|_{r<R} - V_{cr}(\mathbf{r})|_{r<R} \quad (5)$$

is the local short range potential which in general can be considered either as a hole or electron traps. Specifically when the ionic radius of the impurity is larger (smaller) than the ionic radius of host ion, the resulting potential $U_{loc}(r)|_{r<R}$ is expected to capture a hole (electron). In both cases the captured carrier creates the long –range Coulomb potential $-(e^2/(\varepsilon \cdot r))$. $V_{RE}(r)$ is the local short -range potential of the rare earth ion and $V_{cr}(r)$ is the lattice periodic potential, Subscripts $r>R$ and $r<R$ denote the potential outside and inside of the first configurational sphere, respectively, and R is the average distance between the Pr^{3+} ion and ligands.

The lattice relaxation potential, $V_{latt}(\Delta)$ describes the reaction of the lattice ions to the ionization of Pr^{3+} to Pr^{4+} for the case in which a hole is captured or of Pr^{3+} to Pr^{2+} for the case of electron capture. Δ is the shift of the ligands that describes the short distance relaxation in configuration coordinate space.

The change of the electrons number changes the energy of the system by the quantity $\mp \dfrac{C}{R^N}$, where $-$ and $+$ corresponds to the hole and electron trap, respectively. Exponent N depends on the assumed model. For classic electrostatic energy $N=1$, for quantum energy of the electrons in the potential well $N=2$. The crystal field interaction results in $N=5$, whereas the short range quantum repulsion of ligands described by Lennard–Jones potential yields $N=12$. Shift in the configuration coordinate, Δ, that results from lattice relaxation can be calculated by minimization, with respect to Δ, of the lattice energy equal to

$$V_{latt} = \frac{\mp C}{[R+\Delta]^N} + \frac{k\Delta^2}{2}. \qquad (6)$$

In relation (6) k is the elastic constant of the material (related to the bulk modulus). Under the assumption that $\Delta/R \ll 1$ one obtains

$$\Delta = \mp \frac{NC}{kR^{(N+1)}}. \qquad (7)$$

Positive and negative value of Δ correspond to the expansion and compression of the impurity – ligands system, respectively. Finally

$$V_{latt}[\Delta(R)] = -\frac{k}{2}\Delta^2 \mp \frac{C}{R^N} =$$
$$-\frac{N^2C^2}{2kR^{2(N+1)}} \mp \frac{C}{R^N}. \qquad (8)$$

One relates the electron–lattice interaction energy from relation (8) to the configurational coordinate diagram presented in Fig. 3 as follows

$$V_{latt}[\Delta(R)] = \frac{N^2C^2}{2kR^{2(N+1)}} = S\hbar\omega, \qquad (9)$$

where S is Huang –Rhys factor and $\hbar\omega$ is energy of local phonon mode. The energy of the exciton with respect to the ground state of Pr^{3+} is given by:

$$E_{ex} = E_g + E_e \mp \frac{C}{R^N} - S\hbar\omega, \qquad (10)$$

where E_g is band gap energy. The binding electronic energy E_e depends on the local potential and coulomb tail. When local potential is negligible (impurity has the same electronic core and the same ionic radius as the host ion) this energy is given by the effective Rydberg energy $R^*=-13.6(m^*/\varepsilon^2)$eV, where m^* is a free carrier effective mass and ε is static dielectric constant of the material.

To estimate pressure induced changes the energy of trapped exciton one calculate $\dfrac{dE_{ex}}{dp}$. Using relation (10) one obtains:

$$\frac{dE_{ex}}{dp} = \frac{dE_g}{dp} \pm \frac{NC}{R^{N+1}}\frac{dR}{dp} - \frac{dS\hbar\omega}{dp} - \frac{dE_e}{dp}. \qquad (11)$$

Using relation (9) one obtains

$$\frac{dS\hbar\omega}{dp} = \frac{S\hbar\omega}{3B_0}\big[2(N+1) - 6\gamma\big]$$

and

$$\frac{NC}{R^{N+1}}\frac{dR}{dp} = -\frac{N}{3B_0}\frac{C}{R^N}, \qquad (12)$$

where B_0 is local bulk modulus, γ is Grüneisen parameter. Thus depending on N, $\dfrac{dS\hbar\omega}{dp}$ can be smaller or greater than zero. Quantity $\dfrac{dE_e}{dp}$ is rather small when $E_e \approx R^*$. The most important are quantities $\dfrac{N}{3B_0}\dfrac{C}{R^N}$ and $\dfrac{dE_g}{dp}$. The energy of the band gap probably increases with pressure, thus diminishing of the energy of trapped exciton with pressure is related to quantity $-\dfrac{N}{3B_0}\dfrac{C}{R^N}$ (minus means that we have trapped hole). In the case when the exciton is formed by trapped electron and a hole localized at Coulomb electron potential we

would have energetic shift of the exciton state equal to $+\dfrac{N}{3B_0}\dfrac{C}{R^N}$.

4. CONCLUSIONS

We have discussed the influence of pressure on the energies of localized states related to rare earth impurity in dielectric crystals. Especially pressure influences strongly the energies of the states belonging to the excited electronic configuration $4f^{n-1}5d^1$ remaining the states from the ground electronic configuration $4f^n$ almost unchanged. Using the model of impurity trapped exciton system we have argued that pressure can change significantly energies of impurity trapped exciton states.

We have shown that high pressure spectroscopy can be very effective tool for investigation of the nature of localized states related to the rare earth impurity. As en example of high pressure spectroscopy application we have shown the evidence for existence of trapped exciton states in the $LiNbO_3:Pr^{3+}$ and $LiTaO_3:Pr^{3+}$ systems.

REFERENCES

[1] *Phosphor Handbook*, ed.by S. Shionoya and W.M. Yen (CRC Press, Boca Raton 1999).

[2] R. C. Miller and W.A. Norland // *Phys. Rev.* **B2** (1970) 4896.

[3] G.L. Tangonan, M.K. Barnoski, J.F. Lotespeich and A. Lee // *Appl. Phys. Lett.* **30** (1977) 238.

[4] C. M. Combes, P. Dorenbos, C.W.E. van Eijk, C. Pedrini, H. W. Den Hartog, J. Y. Gesland and P.A. Rodnyj // *J. Lumin* **71** (1997) 65.

[5] M. Balcerzyk, Z. Gontarz, M. Moszyñski and M. Kapusta // *J. Lumin.* **87-89** (2000) 963.

[6] P. Dorenbos // *J. Phys. Cond. Matter* **15** (2003) 2645, and references therein.

[7] S. Kück // *Appl. Phys.* **B72** (2001) 515.

[8] P. Dorenbos // *J. Lumin.* **99** (2002) 283.

[9] P. Dorenbos // *J. Lumin.* **91** (2000) 155.

[10] P. Dorenbos // *J. Lumin.* **91** (2000) 91.

[11] E.G. Reut // *Opt. Spektrosk.* **45** (1978) 518.

[12] E.G. Reut // Opt. Spektrosk. **40** (1976) 99.

[13] B. Moine, C. Pedrini and B. Courtois // *J. Lumin.* **50** (1991) 31.

[14] C. Dujardin, B. Moine and C. Pedrini // *J. Lumin.* **54** (1993) 259.

[15] K.L. Bray // *Topics in Current Chemistry* **213** (2001) 1.

[16] M. Grinberg // *Optical Materials* **28** (2006) 24.

[17] C.E. Tyner and H.G. Drickamer // *J. Chem. Phys.* **67** (1977) 4116.

[18] U.R. Rodriguez- Mendoza, G.B. Cunningham, Y.R. Shen and K.L. Bray // *Phys. Rev.* **B. 64** (2001) 195112.

[19] G.B. Cunningham, Y.R. Shen and K.L. Bray // *Phys. Rev.* **B. 65** (2002) 024112.

[20] M. Grinberg, J. Barzowska and T. Tsuboi // *Radiation Effect and Defects* **158** (2003) 39.

[21] G.B. Cunningham, Y.R. Shen and K. L. Bray // *Phys. Rev.* **B. 64** (2001) 195112.

[22] W. Gryk, M. Grinberg, M.-F. Joubert, C. Dujardin, L. Grosvalet and C. Pedrini // *Optical Materials*, in print.

[23] M. Grinberg, Y. R. Shen, J. Barzowska, R. S. Meltzer and K. L. Bray // *Phys. Rev.* **B 69** (2004) 205101.

[24] R.S. Meltzer, H. Zheng, J.W. Wang, W.M. Yen and M. Grinberg // *Phys. Stat. Sol.* **C2** (2005) 284.

[25] C.S. Yoo, H.B. Radousky, N.C. Holmes and N.M. Edelstein // *Phys. Rev.* **B. 44** (1991) 830.

[26] D. B. Gatch, D.M. Boye, Y.R. Shen, M. Grinberg, Y.M. Yen and R.S. Meltzer // *Phys Rev. B.*, in print.

[27] W. Gryk, B. Kukliñski, M. Grinberg and M. Malinowski // *J. Alloy. Comp.* **380** (2004) 230.

[28] W. Gryk, D. Dyl, W. Ryba Romanowski and M. Grinberg // *J. Phys. Cond. Matter* **17** (2005) 5381.

[29] L. Merrill and W.A. Bassett // *Rev. Sci. Instrum.* **45** (1974) 290.